CORROSION AND STRESS CORROSION CRACKING OF 310 STAINLESS STEEL IN SUPERCRITICAL WATER

Y. Behnamian[1], J.L. Luo[1], W.X. Chen[1], W. Zheng[2], D.A. Guzonas[3], Z. Zhou[4], X. Tan[1], D. Mitlin[1],
[1] Department of Chemical and Materials Engineering, University of Alberta, Alberta, Canada
[2] Materials Technology Laboratory, NRCan, Ottawa, Ontario, Canada
[3] Atomic Energy of Canada Limited, Chalk River Laboratories, Chalk River, Ontario, Canada
[4] Universities of Science and Technology Beijing, Beijing, China

Abstract

In the present study, the effect of exposure duration on the corrosion and stress corrosion cracking of 310 stainless steel tube in a supercritical water environment was investigated at 500 ^{o}C in a decreasing dissolved oxygen regime. Oxide films formed three distinct layers after exposure to SCW for 2500 hours. On the outer layer, large magnetite crystals were observed which were tiny on the surface after exposed for 500 hours. In the middle-oxide layer, the concentrations of iron, chromium and nickel were close to those in the substrate. In the inner layer, chromium was enriched while iron was depleted. With increasing exposure duration, the thickness of the oxide layer increased. In the sub-layers of magnetite crystals, some iron-deficient regions were seen because of the selective outward diffusion of iron. Some micro cracks started to form from those iron-deficient regions.

1. Introduction

Water above a temperature of 374.15 ^{o}C and pressure of 22.1 MPa is in the supercritical state. Above the critical point, a supercritical phase is formed [1]. Supercritical water (SCW) acts as a dense gas and exhibits properties significantly different from those of water below the critical point [1-2]. In SCW, the intermolecular structure of water due to hydrogen bond varies leading to large changes in properties such as the dielectric constant and density, which are functions of temperature and pressure [1-3]. At high density, substances with ionic bonds can be dissolved in SCW; however, at low density nonpolar organic substances and gases can be dissolved in SCW. Based on the advantages of a supercritical water reactor (SCWR) compared to current light water reactors, such as high thermal efficiency and simplified design, the SCWR has been selected as a coolant fluid in one of the Generation IV reactor concept.

Due to the widespread use of SCW in many technology areas, a lot of studies have been carried out on the corrosion/oxidation and stress corrosion cracking (SCC) of structural materials in SCW environments containing constant dissolved oxygen (DO) [5-11]. A two-layer oxide typically forms on a metal surface, consisting of a loose outer layer with iron-enrichment and a compact inner layer with chromium and iron enrichment. Gao et al. and Sun et al. studied the corrosion of 316L stainless steel in SCW with 2% H_2O_2 at 24 MPa at temperatures from 400 to 500 ^{o}C [5-7]. Was et al. studied corrosion and SCC of austenitic stainless steel, nickel-based alloys, ferritic–martensitic (F/M) steels and titanium-based alloys using constant extension rate tensile (CERT) [8-11]. They found that F/M steels had quite higher weight gain, while austenitic stainless steels showed less weight gain than F/M steels, but were more prone to oxide spallation. For nickel-base alloys, very little weight gain was observed. The results also showed that increasing the bulk chromium concentration reduced the oxidation rate.

In this paper, the corrosion and SCC of 310 stainless steel (310 SS) tube exposed to a static SCW environment were studied. By sealing water inside the tube and increasing the temperature above the critical point, an SCW environment was produced inside the tube, exposing the inner wall of the tube to SCW. Since no additional oxygen could be added during the tests, the effect was a decreasing dissolved oxygen regime. The trapped SCW provided enough pressure and the required corrosive environment at the inner wall of the 310 SS tubes to study SCC. The main aim of the present work was to provide insight into the effects of exposure duration at 500 ^{o}C with decreasing DO concentration on the corrosion and SCC behaviour of 310 SS.

2. Experimental

The material used in the present study was 310 SS (UNS 31008) in a tube shape with an outer diameter of 0.9525 cm and a wall thickness of 0.1651 cm. The tubes were manufactured based on ASTM-A-213-09, and subjected to a final solution annealing and passivation of the inner side. The chemical composition, in weight percent (wt%), is Fe-0.048C-24.5Cr-20.25Ni-1.17Mn-0.33Si-0.008S-0.023P-0.29Mo. After cutting to a 10 cm length, the tubes were washed with pentane, isopropyl alcohol and acetone in an ultrasonic bath in sequence. The tubes were then filled with a specified amount of deionised (DI) water and the two ends were then sealed with caps made of 316L SS. The temperature in the furnace was set at a constant value of 500 ^{o}C. The pressure of the water inside the tube depended on its density and temperature. Figure 1 shows the relationship between pressure and water density at 500 ^{o}C [12]. According to Figure 1, the pressure of a tube filled with 9.5% volume of DI water is 25 MPa at 500 ^{o}C. This pressure provides the required stress on the inner wall of the tube to study the SCC susceptibility in SCW. Other sets of specimens were heated at 500 ^{o}C for calibration and pressure monitoring. The volume change of the specimens due to creep induced at high temperature and high pressure was measured. X-ray diffraction (XRD) analyses were performed in glancing angel ($\theta = 3^{o}$) using a Cu-Kα radiation source ($\lambda = 1.5406$ Å).

To study the cross section of the oxide films formed on the inner wall, the tubes were cut into small segments and were nickel plated to protect the oxide layers without interfering within analysis. Also, the samples were mounted with epoxy resin and then polished down to 0.5 μm before SEM/EDS investigation. The surface morphologies of the oxide layers on the inner wall of the tube were investigated by secondary electron imaging and the cross-section morphologies were investigated by backscattered electron images at 20 kV.

3. Results and Discussions

3.1 Morphology and Composition of the Oxide Layer Formed on the Inner Wall of 310 SS Tube

Figures 2 (a), (b) and (c) show the topographies of the oxide formed on the inner wall of 310SS tubes before and after exposures of 500 and 2500 hours, respectively. The surface oxide film consisted of crystals of different sizes. After the initial 500 hours exposure, tiny crystals were discretely distributed and did not form a continuous oxide layer. After exposure for 2500 hours, regional crystal growth was observed. Various defects including porosity, micro-cracks and micro-crevices formed between grains can be seen in Figure 2 (c). Figure 3 shows the X-Ray elemental mapping of the oxide; the results revealed that the outer crystal layer contained a higher iron concentration in some regions (blue-concentration of iron, red-concentration of chromium). Based on grazing incidence X-Ray diffraction (GIXRD) investigation, clear magnetite signals were seen; however, the surface was not fully covered by magnetite crystals. Figure 4 shows the XRD pattern of the surface oxide on the inner wall after 2500 hours of exposure. The peaks of magnetite (Fe_3O_4) and an iron-chromium spinel phase ($FeCr_2O_4$) were observed. After exposure, Cr_2O_3 was not observed; Cr_2O_3 could exist at high partial pressure of oxygen base on Fe-Cr-O diagram in 500 °C [21]. However, the 2 μm air-formed passive layer and the decreasing DO regimes decrease the chance for the metal substrate to be exposed to a high partial pressure of oxygen to create Cr_2O_3.

Similar oxide phases were observed on the surface of 12%Cr ferritic/martensitic steel, HCM12A, after exposure to low oxygen-containing (25 ppb) SCW [13]. Cr_2O_3 was not observed to the oxide exposed in low oxygen–containing (25 ppb) SCW; however, it was observed to the oxide exposed in high oxygen–containing (2 ppm) SCW [13]. In the present study, the oxygen concentration was 8 ppm before exposure, but oxygen was not added into the tube during exposure. Therefore, the oxygen partial pressure was high at the beginning of test; and decreased to a very low level during exposure because of consumption of oxygen. A general oxidation mechanism has been suggested; an outer oxide is formed by outward diffusion of iron cations, and the inner oxide is formed by inward diffusion of oxygen anions [14,15]. Following this mechanism, iron cations diffused through the inner oxide layer to the outer oxide layer and reacted with oxygen to form the iron-rich outer oxide layer. At the same time, oxygen anions diffused to the inner oxide layer and reacted mainly with chromium to form the chromium-rich inner oxide layer. Finally, because of the decreasing concentration of DO, oxide growth was probably controlled by the diffusion of cations through the oxide film [22].

3.2 Cross-Section Micrographs of the Oxide Layer and SCC Initiation on the Wall of 310 SS Tubes

Figure 5 shows the cross-section micrographs of the oxide film formed on the inner wall of the tubes before and after 500 and 2500 hours of exposure to SCW environment at 500 °C, analysed using SEM/EDS in backscattered electron mode. The cross-section micrographs and general chemical compositions at different locations of the oxides are shown in the corresponding X-Ray elemental mapping. Before exposure, as shown in Figure 5(a), there was a 2 μm air-formed passive layer which had a composition close to that of the substrate based on the corresponding X-Ray elemental mapping. Figures 5(b) and (c) show the cross-section micrographs of the oxide film formed on the inner wall of the as-received 310 SS after 500 and 2500 hours of exposure in SCW, respectively. After 500 hours of exposure, the thickness of the passive layer increased by an additional 2 μm compared with that of the film before exposure. The 1 μm of outer oxide layer containing discrete iron-rich oxides was formed on top of the inner layer. After 2500 hours of exposure, as shown in Figure 5(c), the oxide had grown more than 6 μm in thickness. The final thickness of the oxide film was about 10 μm. On top of the inner passive layer, distinct iron oxide crystals with the selective diffusion of iron from the inner layer were observed. The corresponding X-Ray elemental mapping shows a three-layer oxide structure: a discontinuous iron-rich outer layer, a middle layer with a composition close to that of the substrate and an inner layer enriched in chromium and depleted in iron.

It has been reported that iron and chromium have higher affinities for oxygen than nickel [16]. The incorporation rate of nickel in the oxide film would be smaller than that of iron and chromium. Therefore, nickel would be expected to become concentrated at the oxide/metal interface [16], which can be seen in the elemental mapping in Figure 5(c). The oxidation behaviour of steel in SCW appears similar to that in a gaseous (steam) environment, which is dominated by molecular processes, and the diffusion rates of cations and anions in the oxide film are the rate-determining processes [17, 18]. Under supercritical conditions, the oxidation process can be affected not only by the oxygen concentration, but also by water. Water could affect the transport processes in the metallic matrix, probably due to hydrogen dissolution [19].

It is well known that most SCC is initiated from localized corrosion sites, which provides local stress concentration. During exposure to SCW, a combination of the hoop stress applied on the inner wall with the corrosion of inner tube wall will initiate cracks. Figure 5(c) shows that after 2500 hours of exposure, cracks several in length were initiated from iron depleted regions. The reactants and products could transport through these micro-defects and corrosion reactions could be accelerated. After long exposure to SCW the thickness of the oxide increased and the tube wall thickness decreased. As a result, the hoop stress applied on the wall increases, which can accelerate SCC.

For short exposure times (500 hours), no significant micrometer cracks were observed. To protect this alloy, maintaining a constant DO concentration may be a possible solution by allowing the formation of thick continuous protective Cr_2O_3 film. Future study is needed to determine the critical DO concentration.

4. Conclusions

In the present work, the effect of exposure duration in a decreasing DO regime on the corrosion and SCC of 310 SS in SCW was investigated using capsule samples and subsequent analysis by SEM/EDS and XRD. The following main conclusions could be drawn:

(1) On the as-received tubes with an air-formed passive layer of 2 μm, for short time exposure (500 hours), a two-layer corrosion film(2 μm in thickness) was formed with an outer layer composed of scattered crystals which were iron-enriched and chromium and nickel-depleted. The composition of these outer oxide crystals was magnetite (Fe_3O_4).

(2) After 2500 hours of exposure, the final thickness of the oxide film was about 10 μm. The oxide had a three-layer structure: a discontinuous iron-rich outer layer, a middle layer with a composition close to that of substrate, and an inner layer enriched in chromium and depleted in iron. For a longer exposure time (2500 hours), the size and quantity of magnetite crystals was an order of magnitude larger than those after exposure for 500 hours.

(3) Increased passive layer had more cracks that accelerated the selective diffusion of iron to the outer layers and oxygen to inner layer, indicating that the passive layer was not protective.

(4) The as-received inner surface of the 310 SS tube was susceptible to SCC in decreasing DO regime.

5. Acknowledgments

The authors gratefully acknowledge financial support from NSERC/NRCAN/AECL CRD program.

6. References

[1] P. Kritzer, "Corrosion in high-temperature and supercritical water and aqueous solutions: a review", Journal of Supercritical Fluid, Vol.29, Iss.1-2, 2004, pp.1-29.

[2] D. Broll, C. Kaul, A. Kramer, P. Krammer, T. Richter, M. Jung, H. Vogel, P. Zehner, "Chemistry in supercritical water", Angew Chem. International Edition, Vol.38, Iss.20, 1999, pp.2998-3014.

[3] H. Ohtaki, T. Radnai, T. Yamaguchi, "Structure of water under subcritical and supercritical conditions studied by solution X-ray diffraction", Chemical Society Reviews, Vol.26, 1997, pp.41-51.

[4] D. Squarer, T. Schulenberg, D. Struwe, Y. Oka, D. Bittermann, N. Aksan, C. Maraczy, R. Kyrki-Rajamaki, A. Souyri, P. Dumaz, "High performance light water reactor", Nuclear Engineering and Design, Vol.221, Iss.1-3, 2003, pp.167-180.

[5] X. Gao, X.Q. Wu, Z.E. Zhang, H. Guan, E.H. Han, "Characterization of oxide films grown on 316L stainless steel exposed to H_2O_2-containing supercritical water", Journal of Supercritical Fluids, Vol.42, Iss.1, 2007, pp.157-163.

[6] M.C. Sun, X.Q. Wu, Z.E. Zhang, E. H. Han, "Oxidation of 316 stainless steel in supercritical water", Corrosion Science, Vol.51, 2009, pp.1069-1072.

[7] M.C. Sun, X.Q. Wu, E.H. Han, J.C. Rao, "Microstructural characteristics of oxide scales grown on stainless steel exposed to supercritical water", Scripta Materialia, Vol.61, Iss.10, 2009, pp.996-999.

[8] G.S. Was, P. Ampornrat, G. Gupta, S. Teysseyre, E.A. West, T.R. Allen, K. Sridharan, L. Tan, Y. Chen, X. Ren, C. Pister, "Corrosion and stress corrosion cracking in supercritical water", Journal of Nuclear Materials, Vol.371, Iss.1-3, 2007, pp.176-201.

[9] S. Teysseyre, G.S. Was, "Stress corrosion cracking of austenitic alloys in supercritical water", Corrosion, vol. 62, 2006, pp.1100-1116.

[10] Q.J. Peng, S. Teysseyre, P.L. Andresen, G.S. Was, "Stress corrosion crack growth in type 316 stainless steel in supercritical water", Corrosion, Vol.63, 2007, 1033-1041.

[11] S. Teysseyre, Z. Jiao, E. West, G.S. Was, "Effect of irradiation on stress corrosion cracking in supercritical water", Journal of Nuclear Materials, Vol.371, Iss.1-3, 2007, pp.107-117.

[12] E.W. Lemmon, M.O. McLinden, D.G. Friend, "Thermophysical properties of fluid systems" in NIST Chemistry WebBook, NIST Standard Reference Database Number 69, Eds. P.J. Linstorom and W.G. Mallard, National Institute of Standards and Technology, Gaithersburg MD, 20899, http://webbook.nist.gov, (retrieved March 24, 2010)

[13] L. Tan, Y. Yang, T.R. Allen, "Oxidation behaviour of iron-based alloy HCM12A exposed in supercritical water", Corrosion Science, Vol.48, 2006, pp.3123-3138.

[14] A.D. Siwy, T.E. Clark, A.T. Motta, “Transmission electron microscopy of oxide development on 9Cr ODS steel in supercritical water”, Journal of Nuclear Materials, Vol.392, Iss.2, 2009, pp.280-285.

[15] J. Bischoff, A.T. Motta, R.J. Comstock, “Evolution of the oxide structure of 9CrODS steel exposed to supercritical water”, Journal of Nuclear Materials ,Vol.392, Iss.2, 2009, pp.272-279.

[16] X. Ren, K. Sridharan, T.R. Allen, “Corrosion of ferritic-martensitic steel HT9 in supercritical water”, Journal of Nuclear Materials, Vol.358, Issues 2-3, 2006, pp.227-234.

[17] D.D. Macdonald, “Effect of pressure on the rate of corrosion of metals in high subcritical and supercritical aqueous systems”, Journal of Supercritical Fluids, Vol.30, Issue.3, 2004, Pages 375-382.

[18] Y. Yi, B. Lee, S. Kim, J. Jang, “Corrosion and corrosion fatigue behaviours of 9Cr steel in a supercritical water condition”, Materials Science and Engineering, Vol.429, Iss.1-2, 2006, pp.161-168.

[19] E. Essuman, G.H. Meier, J. Zurek, M. Hansel, W.J. Quadakkers, “The effect of water vapour on selective oxidation of Fe–Cr alloys”, Oxidation of Metals, Vol.69, 2008, pp. 143-162.

[20] I.G. Wright, B.A. Pint, “An assessment of the high-temperature oxidation behaviour of Fe–Cr steels in water vapour and steam”, Proceeding of Corrosion 2002 Paper No 2377, Denver, Colorado, USA, 2002 April 7-11.

[21] P. Ampornrat, C.B. Bahn, G.S. Was, “ Corrosion and stress corrosion cracking of ferritic-martensitic alloys in supercritical water”, Proceeding of the 12th International Conference on Environmental Degradation of Materials in Nuclear Power System-Water Reactors, Salt Lake City, Utah, United States, 2005 August14-18.

[22] G.S. Was, T.R. Allen, “Time, temperature, and dissolved oxygen dependence of oxidation of austenitic and ferritic-martensitic alloys in supercritical water”, Proceeding of ICAPP ‘05, Seoul, Korea, 2005 May15-19.

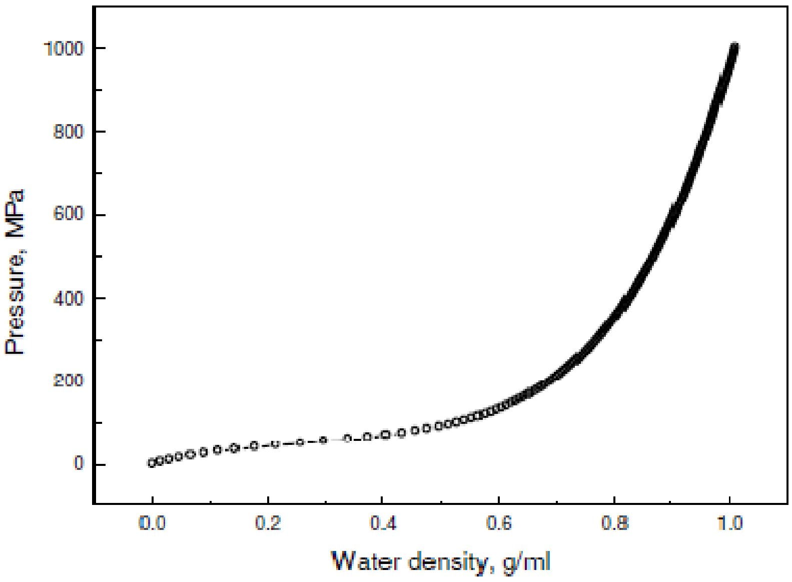

Figure 1 Pressure vs. density of water at 500 °C. [12]

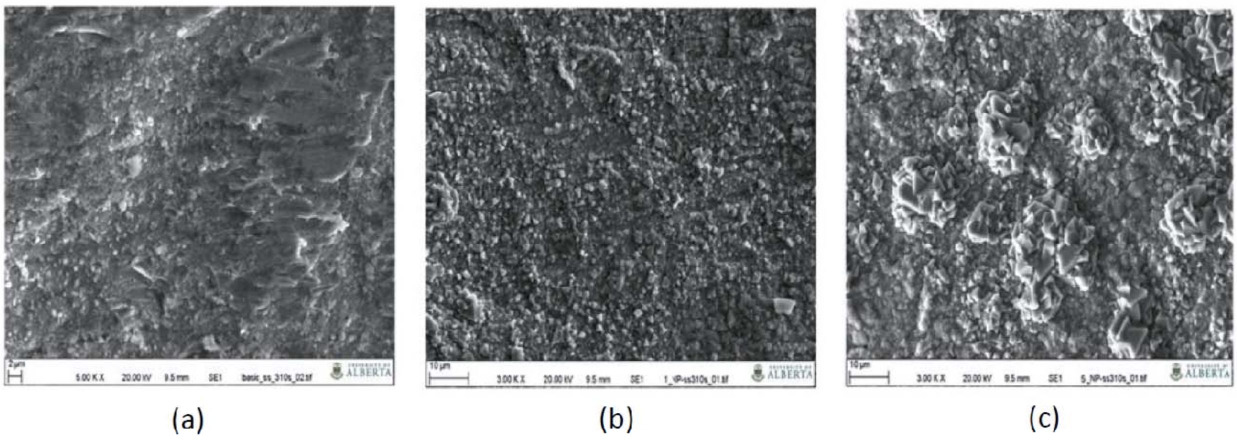

Figure 2 SEM micrographs of the oxide formed on the inner wall of 310 SS after 0 (a), 500 (b) and 2500 hours (c) of exposure to SCW.

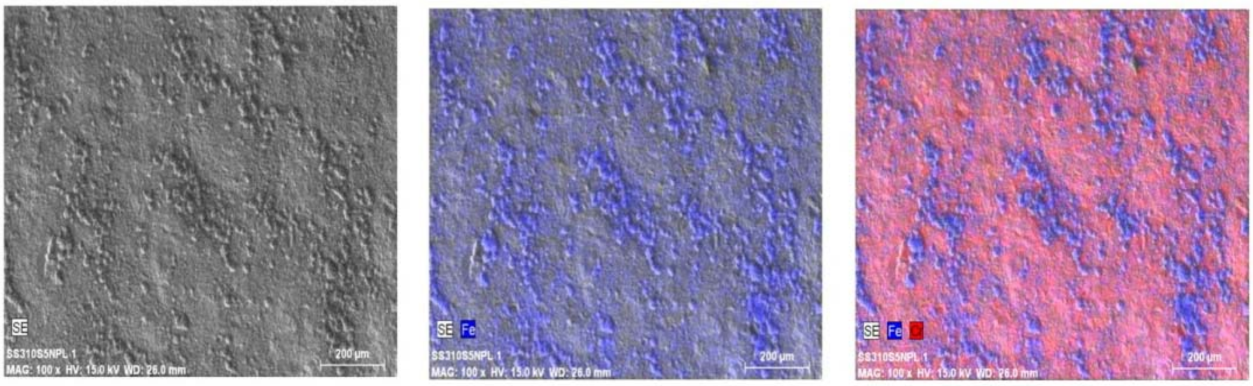

Figure 3 SEM micrographs of the oxide formed on the inner wall of 310 SS after 2500 hours of exposure to SCW at lower magnification (blue-concentration of oxygen, red-concentration of chromium).

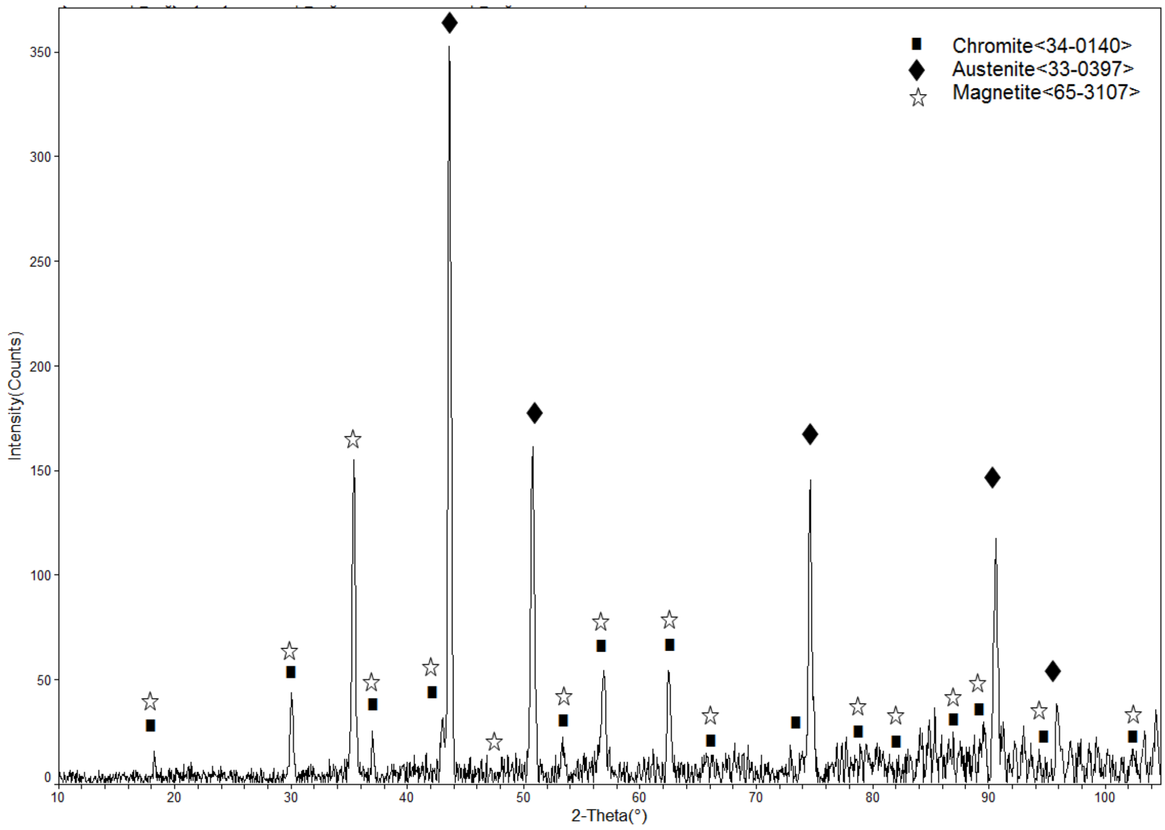

Figure 4 XRD pattern of the surface oxide formed on the inner wall of 310 SS after 2500 hours of exposure to SCW.

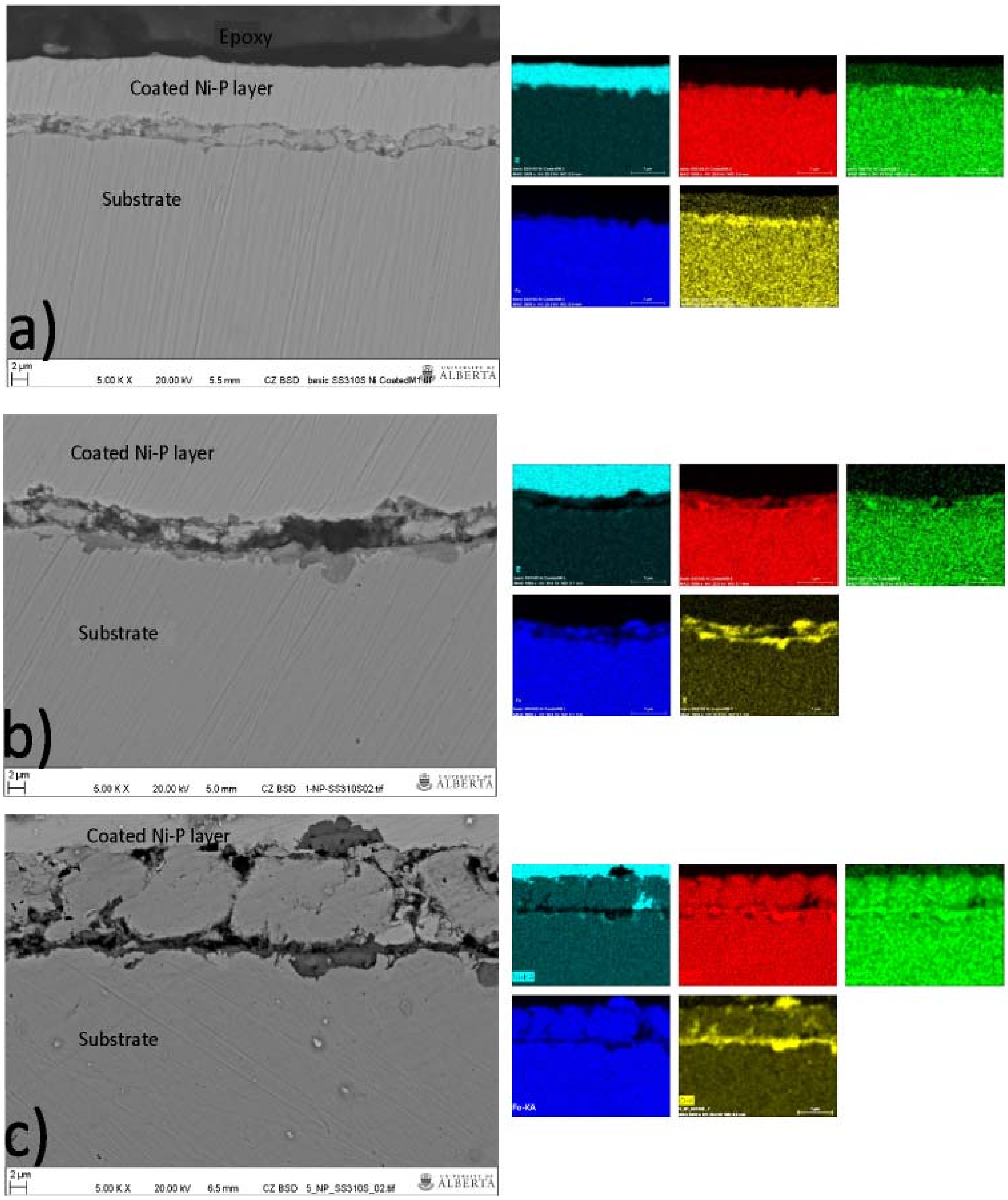

Figure 5 Cross-section micrographs of the oxide film formed on the inner wall of the 310 SS under as-received condition after 0 (a), 500 (b), 2500 (c) hours of exposure to SCW with X-ray elemental mapping at 500 °C (yellow-oxygen concentration, blue-iron concentration, green-manganese concentration, red-chromium concentration, turquoise- nickel concentration).